The Journal of Experimental Biology 204, 325–335 (2001)
Printed in Great Britain © The Company of Biologists Limited 2001
JEB3078

STRUCTURAL FLEXIBILITY OF THE INTESTINE OF BURMESE PYTHON IN RESPONSE TO FEEDING

J. MATTHIAS STARCK* AND KATHLEEN BEESE

Institute of Systematic Zoology and Evolutionary Biology, Friedrich-Schiller-Universität Jena, Erbertstraße 1, D-07743 Jena, Germany

*e-mail: starck@pan.zoo.uni-jena.de

Accepted 23 October 2000; published on WWW 3 January 2001

Summary

The small intestine of Burmese pythons, *Python molurus bivittatus*, undergoes a remarkable size increase shortly after feeding. We studied the dynamics, reversibility and repeatability of organ size changes using noninvasive imaging techniques. We employed light and electron microscopy, flow cytometry and immunohistology to study the cytological mechanisms that drive the size changes of the small intestine. Within 2 days of feeding, the size of the small intestine increased to up to three times the fasting value. The size changes were fully reversible and could be elicited repeatedly by feeding. These enormous size changes were possible because the mucosal epithelium of the small intestine is a transitional epithelium that allows for considerable size changes without cell proliferation. Histological evidence suggested that a fluid pressure-pump system (lymphatic, blood pressure) was the driving force that inflated the intestinal villi. The rates of cell proliferation were not elevated immediately after feeding but peaked 1 week later when small intestine size was already declining. In contrast to the current paradigm, we suggest that the small intestine is not part of the previously proposed 'pay-before-pumping' model. Instead, the size of the python's small intestine may be upregulated without major metabolic investment. It can occur even if the individual is energetically exhausted. An evolutionary perspective of the transitional epithelium mechanism suggests superior functionality compared with the pay-before-pumping model because it allows for long periods of fasting and depletion of energy reserves, while still enabling the snake to digest prey and absorb nutrients.

Key words: phenotypic flexibility, gastrointestinal tract, nutrition, functional anatomy, Burmese python, *Python molurus bivittatus*.

Introduction

Current paradigms of animal design (Weibel et al., 1998) presume that the size and function of an organ system are balanced by the costs of running the system. Because maintenance of tissue costs metabolic energy, any capacity of an organ in excess of the actual demand ought to be reduced. Conversely, insufficient capacity should be upregulated to exploit the full extent of available resources. These ideas provide a theoretical framework for hypotheses about matching between the loads and capacities of an organ system. The predictions are (i) that adjustment of the digestive tract to feeding conditions should be rapid to minimize periods of mismatching; (ii) that responses should be fully reversible and frequently repeatable; (iii) that responses should match demands and (iv) that the costs of flexibility should be below the costs of maintenance.

As pointed out previously (Secor, 1995; Secor and Diamond, 1995; Secor and Diamond, 1997; Secor and Diamond, 1998; Piersma and Lindström, 1997; Starck, 1999), the python's digestive tract is an interesting system with which to study physiological and morphological regulation of organ size and function. After long periods of fasting, pythons swallow prey that may be of similar body mass to the snakes themselves. Such intermittent feeding episodes impose fluctuating functional demands on the digestive system. After feeding, the gastrointestinal system has to digest the meal, absorb nutrients and transport the digesta along the intestine. On average, digestion, absorption, excretion and defecation occur within 8–14 days of food intake. Within a few days of feeding, levels of enzyme activities and nutrient uptake rates increase 6–26 times compared with fasting values, and metabolic rates peak at 17 times the resting value (Secor et al., 1994). Overgaard et al. report a postprandial increase in metabolic rate in Burmese pythons by a factor of only 3.2 (Overgaard et al., 1999). Within 24 h, the masses of the liver and the small intestine increase to more than twice the fasting values (Secor et al., 1994). When fasting, the digestive tract is reduced. Estimates of the energetic value of a full meal and the increase in metabolic rate after feeding associated with digestion (specific dynamic action, SDA) in pythons led to the suggestion that the python's intestine works like a USA gasoline station, i.e. applies the 'pay-before-pumping' principle (Secor and Diamond, 1995). They estimated that

SDA in pythons is fuelled by an equivalent of 30 % of the ingested energy. They suspected that the majority of that energy was invested into turning on the absorptive machinery and producing a new intestine (pay) before the meal could be absorbed (pumping). Because the energy cannot come from the meal, they hypothesized that it arises from mobilization of the snake's energy resources. Secor et al. and Secor and Diamond stated that mucosal growth and atrophy provide the mechanisms for up- and downregulation of organ size (Secor et al., 1994; Secor and Diamond, 1995; Secor and Diamond, 1998). It remained unclear what cellular mechanisms drive organ growth. Hypertrophy (i.e. organ growth through increase in cell size) or hyperplasy (i.e. organ growth through increase in cell number, cell proliferation) are the two mechanisms that are conventionally considered to change organ size. Implicitly, increases in the wet and dry mass of intestinal organs (growth) associated with high energy expenditure suggest tissue production, and atrophy suggests cellular atrophy, i.e. apoptosis (Cossins and Roberts, 1996). However, for organ size to increase by a factor of 3 within 24–48 h by cell proliferation, there must exist an extremely short cell cycle or mitotic activity of almost all the cells of that organ.

In this study, we analyze the reversibility and repeatability of the flexible response of the snake's small intestine and the cellular mechanisms underlying up- and downregulation of organ size changes. The repeatability and reversibility of small intestine size changes of individuals under fluctuating conditions were studied by repeated ultrasonography. Measurements of the thickness of the mucosa (i.e. lamina propria mucosae and lamina epithelialis mucosae) provide a functionally relevant gross morphological estimate of the functional capacity of the small intestine (Starck and Burann, 1998). Histological and immunohistochemical techniques were employed to study the flexible responses at the level of tissues and cells. The epithelial surface area is the most important morphological variable that determines nutrient uptake capacity. The absorptive surface area depends on the number and length of intestinal villi that reach into the lumen of the gut and on the number and length of the microvilli of each enterocyte. Therefore, we measured the length of the microvilli, the length of the intestinal villi, the thickness of the muscle layer and the circumference of the gut to obtain a functional morphological estimate of the capacity of the intestine to absorb digesta.

The pay-before-pumping hypothesis predicts that stored energy is used to fuel the upregulation of gut size and function, prior to the absorption of ingested energy. Some of that upregulation involves tissue growth. The period of downregulation should be accompanied by reduced rates of cell proliferation or high rates of cell death (apoptosis). To test whether size changes of the small intestine are based on changes in cell proliferation rates and programmed cell death in the small intestine of pythons at different times after feeding and during fasting, we quantified cell proliferation in histological sections by observing and counting mitotic structures. In addition, we used flow cytometry to study the proportion of cycling, noncycling, and apoptotic cells in biopsy samples.

Materials and methods

Animals

We studied two groups of snakes kept under the same conditions. Group 1 was used for repeated noninvasive measurements of small intestine size and for microbiopsies. These animals were alive and in good condition at the end of the study. Group 2 was used for histological investigations.

Group 1: in 1997, five (three females, two males) 9-month-old (body length 100–125 cm; body mass 570–780 g) Burmese pythons (*Python molurus bivittatus* Kuhl) were purchased from a commercial reptile farm in Germany (permit no. 2384\96 V.07.11.9; CITES no. 3006\062348-52). During the first year of the study, the animals were kept in individual cages (100 cm×50 cm×50 cm) at room temperature (25 °C), 50 % humidity and with a 12 h:12 h L:D photoperiod. Later, all five animals shared a cage (400 cm×120 cm×120 cm) under the same conditions. The size responses of the small intestine of these animals were studied over a period of 890 days using ultrasonography. Group 2: six 3-month-old Burmese pythons (40–80 cm; 190–650 g; sex not determined) were purchased in 1998 from the same source. These animals were kept in individual cages for 6 months under the conditions described above and were then processed for histology. When these animals were killed at an age of 9 months, they had experienced repeated feedings and had shown up- and downregulation of organ size (as measured by ultrasonography) identical to the snakes in group 1. We therefore concluded that the histological mechanisms described here do not change during postnatal ontogeny.

Feeding

Meal size was 30–50 % of the snake's body mass. Animals were fed at variable intervals between 12 and 125 days, as indicated in the figures. We fed live or dead mice (30–60 g), rats (250–500 g) or rabbits (1500–4000 g) according to the size of the snake and the availability of the food.

Imaging

Ultrasonography

We used an ophthalmological ultrasonography system (I^3 Innovative Imaging Inc., Sacramento, CA, USA), equipped with a 10 MHz sector scanner in B-mode (scan angle 52 °; scan speed 28 frames s^{-1}; frequency 10 MHz, dynamic range 90 dB; resolution 0.15 mm axially, 0.2 mm laterally; image depth 45 mm; gray-scale 256 shades; cross-vector scale calibrated to 1550 m s^{-1}). The applicator surface was concave. All animals were tame, and ultrasonography was performed without sedation. Ultrasonic gel was used for coupling the applicator to the surface of the animal. Evaluations of ultrasonography as a tool for studying morphometric changes of the gastrointestinal tract have been carried out previously

(Hildebrandt et al., 1998; Starck and Burann, 1998; Dietz et al., 1999; Starck et al., 2001).

Histology

The six animals bought in 1998 (group 2) were killed at the age of 9 months by an overdose of sodium pentabarbitol. Three animals were killed in fasting condition, and three were killed 2 days after feeding on a meal of 50 % their own body mass. Tissue samples from the anterior part of the small intestine were preserved immediately for histology.

Light microscopy

Tissue samples were preserved in 5 % paraformaldehyde in 0.1 mol l^{-1} phosphate buffer (pH 7.4) at 4 °C for at least 48 h. Before embedding in hydroxyethyl methacrylate (Historesin), tissue samples were washed in buffer and dehydrated through a graded series of ethanol to 96 % ethanol. Methacrylate-embedded material was sectioned into short series of 50 sections per sample (section thickness was 2 μm), mounted on slides and stained.

Stains and histochemistry

Methacrylate sections were stained with Methylene Blue/Thionin. An immunohistochemical stain for cytoplasmatic transglutaminase and an *in situ* nick-end labelling technique with bromodeoxyuridine (see Aschoff et al., 1996; Aschoff and Jirikowski, 1997) were applied to detect apoptotic cells in histological sections. Mouse intestinal tissue was used as a positive control on the same slide as the snake tissue.

Alkaline phosphatase is a non-specific enzyme catalyzing the hydrolysis of organic phosphate esters. On a rough scale, it is indicative of the enzymatic activity of the brush border. The topographic distribution and activity of brush-border alkaline phosphatase were examined with the azo-dye coupling technique (Bancroft and Stevens, 1996). Microphotographs were taken with a Zeiss Axioplan photomicroscope on Agfa Pan 25 film.

Transmission electron microscopy

Tissue samples for transmission electron microscopy were preserved in 2.5 % glutaraldehyde in 0.1 mol l^{-1} phosphate buffer (pH 7.4) for 48 h at 4 °C and subsequently treated with 1 % osmium tetroxide in phosphate buffer for 1.5 h. Dehydration, embedding in epon resin, sectioning (thickness 0.09 μm) and staining with uranyl acetate/lead citrate followed standard protocols for transmission electron microscopy. Sections were studied using a Leo 906E, Leo Electron Microscopy Ltd, Cambridge, UK.

Microbiopsy and flow cytometry

Tissue samples were taken from the small intestine of pythons in deep anaesthesia by transrectal endoscopic microbiopsy during routine diagnostic procedures on snakes. Biopsies were taken from snakes in fasting condition and 2, 4, 7 and 10 days after feeding. We took two tissue samples per day and animal, but each animal underwent microbiopsy only once during a feeding cycle. Microbiopsies were taken during three successive feeding intervals. Biopsy material was frozen immediately in liquid nitrogen and stored at −80 °C until processed. For flow cytometry, biopsies were thawed and treated with 0.75 % Triton-X 100 in 0.01 mol l^{-1} Tris-HCl buffer at pH 7.4 to extract nuclei from the tissue. Isolated nuclei were stained with propidium iodide for DNA content, and their fluorescence was measured in a Facs Calibur flow cytometer (Becton Dickinson & Co., San Jose, CA, USA).

The relative amount of DNA in the nuclei is indicative of the cell cycle phase of the cell. Nuclei containing between the normal and double the normal DNA content are considered to be S-phase cells. Nuclei containing twice the normal DNA content may be G2-phase or mitotic cells. Because flow cytometry did not discriminate nuclear size, counts of G2-phase and mitotic cells may be inflated by some G1-phase nuclei sticking together. Therefore, we refer to the proportion of S-phase cells as indicative of the proliferation activity of the tissue. The fraction of cells containing less than the normal DNA content is considered to represent apoptotic cells, but it may also contain fragments of nuclei.

Morphometry

Body mass measurements were taken on an electronic balance (Metzler, Germany) at 0.01 g. Ultrasonographs were saved on disk and read into a personal computer. We used SigmaScanPro (version 4.0, Jandel Scientific, SPSS Inc., Chicago, USA) for image analysis and morphometric data acquisition. From ultrasonographs, we measured the thickness of the mucosa of the small intestine.

Histological sections were studied using a Jenaval research microscope (Zeiss, Jena) equipped with a video camera and connected to the computer-based image-analysis and morphometry system. From each section, we measured the circumference of the gut, the thickness of the muscle layer (tunica muscularis) and the height of the villi from the muscle layer to the top of the villi. We measured 10 sections per tissue sample and took 15 measurements of thickness of muscle layer and height of villi per section. The length of the microvilli was measured using the online measurement option Leo 906E.

Statistical analyses

Approximately 60 000 ultratrasonographs were recorded and analyzed. Values are given as means ± S.D. (*N*=sample size). Repeated-measures analysis of variance (ANOVA) was performed within the framework of general linear models to account for reduced degrees of freedom through repeated measurements on the same individuals. Alternatively, we used a factorial ANOVA with individual means. The $P<0.05$ level was considered significant. All statistical procedures were performed using SAS version 6.5, SAS-Institute Inc., Cary, NC, USA.

Results

Body mass

During the course of this study and under the given feeding and temperature conditions, the snakes in group 1 grew from an average of 600 to 7500 g and from 0.6 m in body length (snout to anus) to more than 3 m. Body mass peaked after each feeding. When these peaks were omitted, mean body mass increased by 876 g per 100 days. The snakes did not reach sexual maturity or adult body size. For comparison, mean adult body size of Burmese pythons is approximately 6.5 m in females and 4.5 m in males.

Morphometry

Thickness of the intestinal mucosa

Repeated ultrasonographic measurements of snakes in group 1 showed that the thickness of the intestinal mucosa increased significantly within 24 h after feeding. Within 48–72 h of feeding, it peaked at an average of 300 % of fasting size. The decline was slower (Fig. 1), and 10 days after feeding mucosa thickness was on average 10 % thicker than before feeding. Repeated-measures ANOVA (with measurements of mucosa thickness as repeats within individuals) showed a highly significant effect of feeding on mucosa thickness (d.f.=7, F=56.51, P=0.01). Individual differences were not significant (d.f. 4, F=1.5, P=0.4). If mean values of mucosa thickness of fasting and digesting individuals were entered into the analysis and the eight feeding events were considered to be repeated measures of the same individual, the results were consistent with the previous analysis: 'feeding' had a highly significant effect (d.f.=7; F=6.6, P=0.001) on mucosa thickness; 'individual' did not have a significant effect. A *post-hoc* comparison among means of mucosa thickness (Ryan–Einot–Gabriel–Welsch multiple F-test, SAS 6.5, proc GLM, REGWF statement) showed that responses to repeated feeding events were uniform and that post-feeding peak values did not differ among the eight feeding events. Also, mucosa thickness always returned to the same fasting size (Fig. 1A). Examination of individual patterns of responses showed a slow and continued decline in the mucosa thickness during the entire fasting period. This pattern was found consistently in all snakes (Fig. 1B).

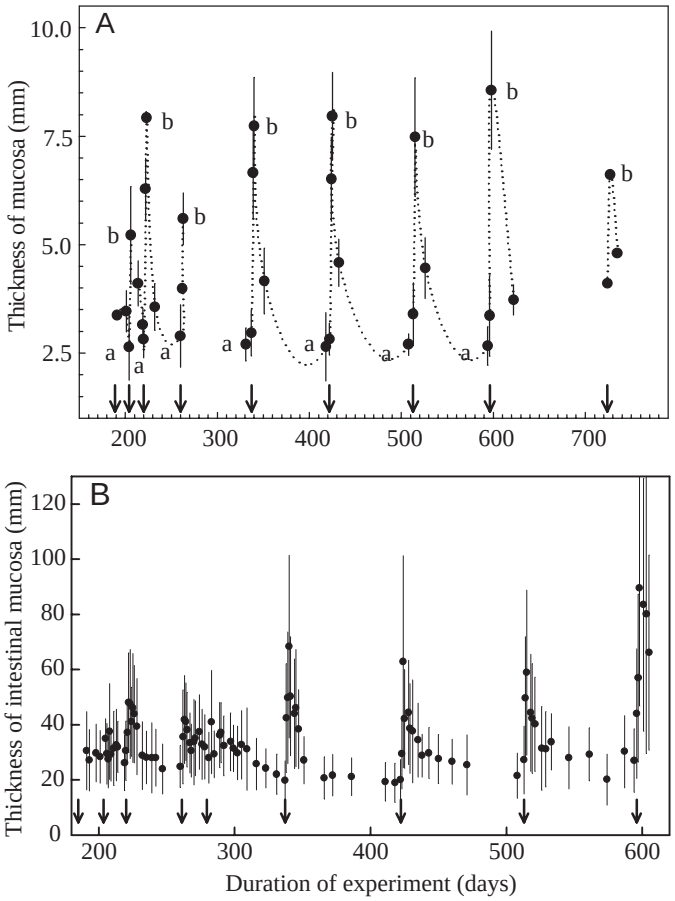

Fig. 1. Flexible response of the thickness of the intestinal mucosa in response to feeding as measured from ultrasonographs. Arrows indicate feeding events. (A) Values are mean ± S.D. from five snakes; for clarity of presentation, only measurements from the day before feeding and 1 day, 2 days and 10 days after feeding have been plotted. Ryan–Einot–Gabriel–Welsch multiple range test for *post-hoc* comparisons among means comparing digesting and fasting snakes; means labelled with different letters are significantly different (α=0.05). (B) Changes in mucosa thickness in an individual snake (P1) to demonstrate individual organ size changes. Values are means ± S.D. from daily measurements on the snake.

Circumference of the small intestine

The circumference of the small intestine (Fig. 2), measured on histological slides (group 2 snakes), was on average

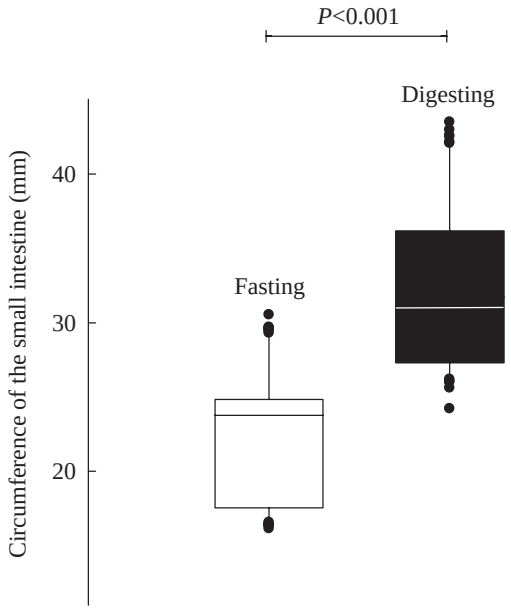

Fig. 2. The circumference of the gut of fasting (67 measurements on N=3 snakes) and digesting (61 measurements on N=3 snakes) pythons. Box-and-whisker plot, with horizontal lines showing the 25th, 50th and 75th percentiles as lines on the box, the fifth and the 95th percentiles as error bars (whiskers) and outliers (circles).

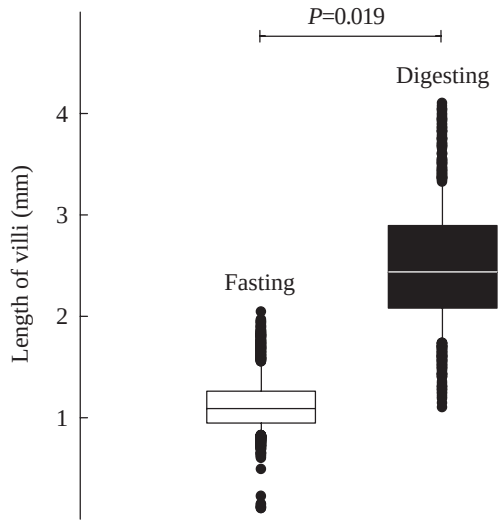

Fig. 3. The length of intestinal villi in the small intestine of fasting (871 measurements on *N*=3 snakes) and digesting (1597 measurements on *N*=3 snakes) pythons. Measurements were made from the tip of the villus to the inner border of the lamina muscularis mucosae. Box-and-whisker plot, with horizontal lines showing the 25th, 50th and 75th percentiles as lines on the box, the fifth and the 95th percentiles as error bars (whiskers) and outliers (circles).

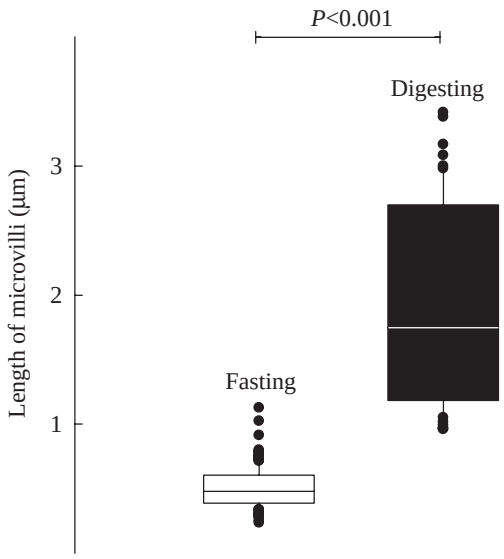

Fig. 4. Length of microvilli of small intestinal enterocytes of fasting (56 measurements on *N*=3 snakes) and digesting (178 measurements on *N*=3 snakes) pythons. Measurements were taken from tip of the microvilli to the apical plasma membrane of the enterocyte body, and only from those microvilli that were sectioned longitudinally. Box-and-whisker plot, with horizontal lines showing the 25th, 50th and 75th percentiles as lines on the box, the fifth and the 95th percentiles as error bars (whiskers) and outliers (circles).

21.8±4.37 mm (*N*=3) in the fasting snakes and 34.02±7.3 mm (*N*=3) in the digesting snakes. The differences between fasting and digesting snakes were highly significant (one-way ANOVA, d.f.=1,5; *F*=56.2; *P*<0.001).

Thickness of muscle layer

On average, the thickness of the muscle layer (tunica muscularis) was 0.23±0.08 mm (*N*=3) in the fasting snakes and 0.29±0.13 mm (*N*=3) in the digesting snakes. The mean values of the two groups did not differ significantly (one-way ANOVA; d.f.=1,4; *F*=0.295; *P*=0.16).

Length of intestinal villi

The length of intestinal villi (Fig. 3) was on average 1.23±0.28 mm (*N*=3) in fasting snakes and 2.82±0.67 mm (*N*=3) in digesting snakes. The differences were statistically significant (one-way ANOVA of means of individuals with food as the main effect; d.f.=1,4; *F*=14.29; *P*=0.019). We also calculated a nested model of 'section', 'tissue sample' and 'individual' in 'food'. 'Individual' and 'tissue sample' were significant effects. This indicates that villus length may also depend on differences between individual snakes and gut topography. The component of variance explained by the effects of 'food' was 78.9 %. Only 7.2 % of the total variance was associated with effects of 'individual' and 2 % with 'tissue sample'.

Length of microvilli

The length of microvilli (Fig. 4) averaged 0.51±0.15 μm (*N*=3) in fasting snakes and 1.93±0.76 μm (*N*=3) in digesting snakes. Microvilli were significantly longer after feeding than during fasting (repeated-measures ANOVA; *P*<0.001; d.f.=1,24; *F*=54.7). We found a marginally significant effect of individual (repeated-measures ANOVA; d.f.=1, 2; *F*=3.56; *P*=0.036), but no significant interactions between the effects of feeding and individual.

Histology

The epithelial lining of the small intestine of digesting pythons (group 2) showed the typical features of a functional mucosal epithelium as known from many other vertebrates. The mucosal epithelium is a single-layered columnar epithelium. The nuclei of the enterocytes are located in the basal third of the cell (Fig. 5A). The enterocytes are relatively large, bear a conspicuous brush border and include a large number of vesicles (Fig. 5B). As revealed by transmission electron microscopy, the vesicles are not surrounded by membranes and are therefore probably lipid droplets. In some cells, these droplets were so numerous and so large that the nucleus was deformed (Fig. 5C). The microvilli of the brush border were prominent (Fig. 5D). Light microscopic sections showed a high activity of alkaline phosphatase in the brush border of digesting snakes (Fig. 5E). The microvilli were covered by a prominent surface coat and contained the characteristic core of actin filaments. Actin filaments were rooted in a well-developed terminal web. Neighbouring enterocytes were connected by tight junctions (circular desmosomes) at their apical end. However, digesting pythons had large intercellular spaces between the enterocytes (Fig. 5B), providing wide channels for paracellular transport.

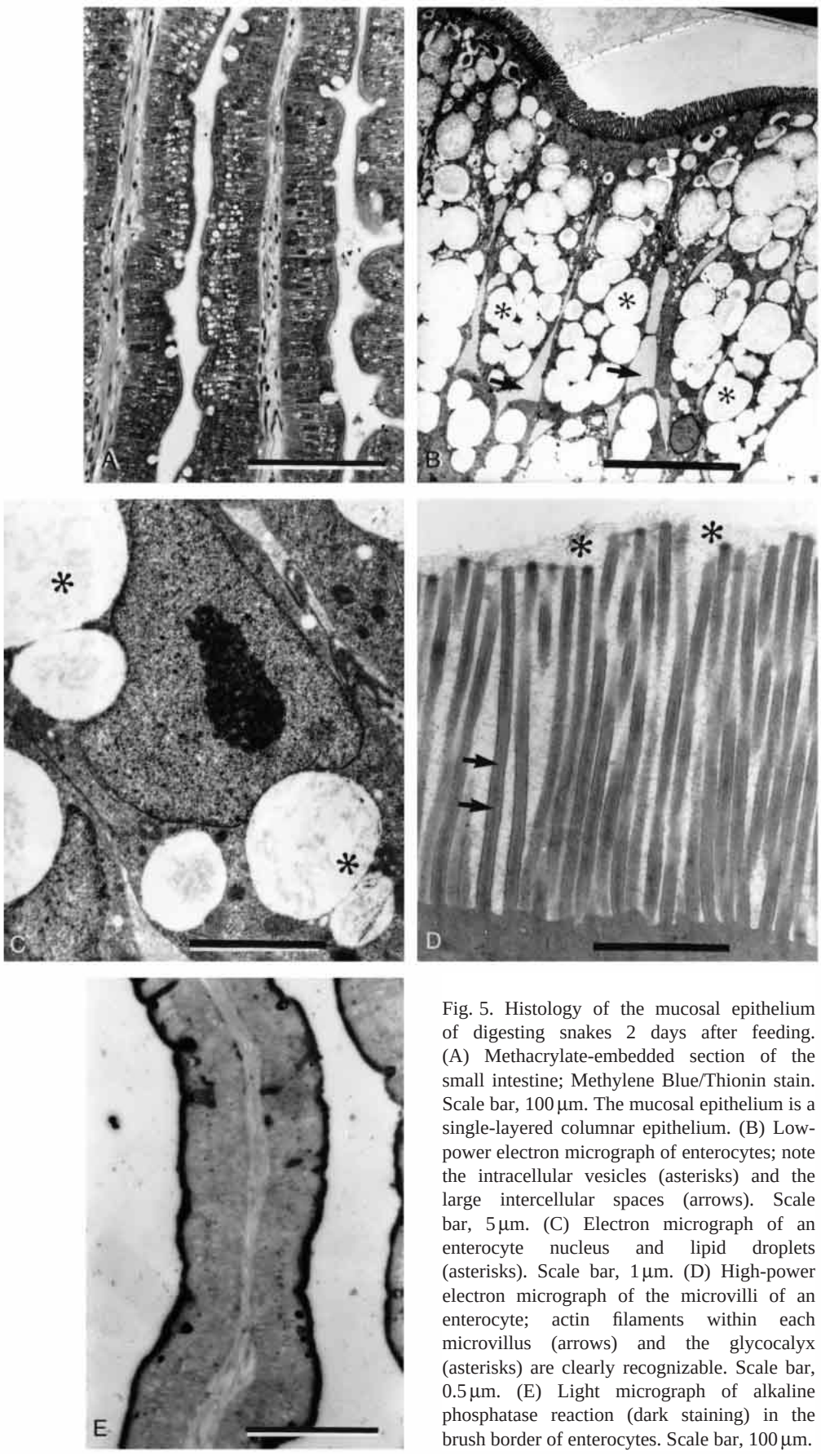

Fig. 5. Histology of the mucosal epithelium of digesting snakes 2 days after feeding. (A) Methacrylate-embedded section of the small intestine; Methylene Blue/Thionin stain. Scale bar, 100 μm. The mucosal epithelium is a single-layered columnar epithelium. (B) Low-power electron micrograph of enterocytes; note the intracellular vesicles (asterisks) and the large intercellular spaces (arrows). Scale bar, 5 μm. (C) Electron micrograph of an enterocyte nucleus and lipid droplets (asterisks). Scale bar, 1 μm. (D) High-power electron micrograph of the microvilli of an enterocyte; actin filaments within each microvillus (arrows) and the glycocalyx (asterisks) are clearly recognizable. Scale bar, 0.5 μm. (E) Light micrograph of alkaline phosphatase reaction (dark staining) in the brush border of enterocytes. Scale bar, 100 μm.

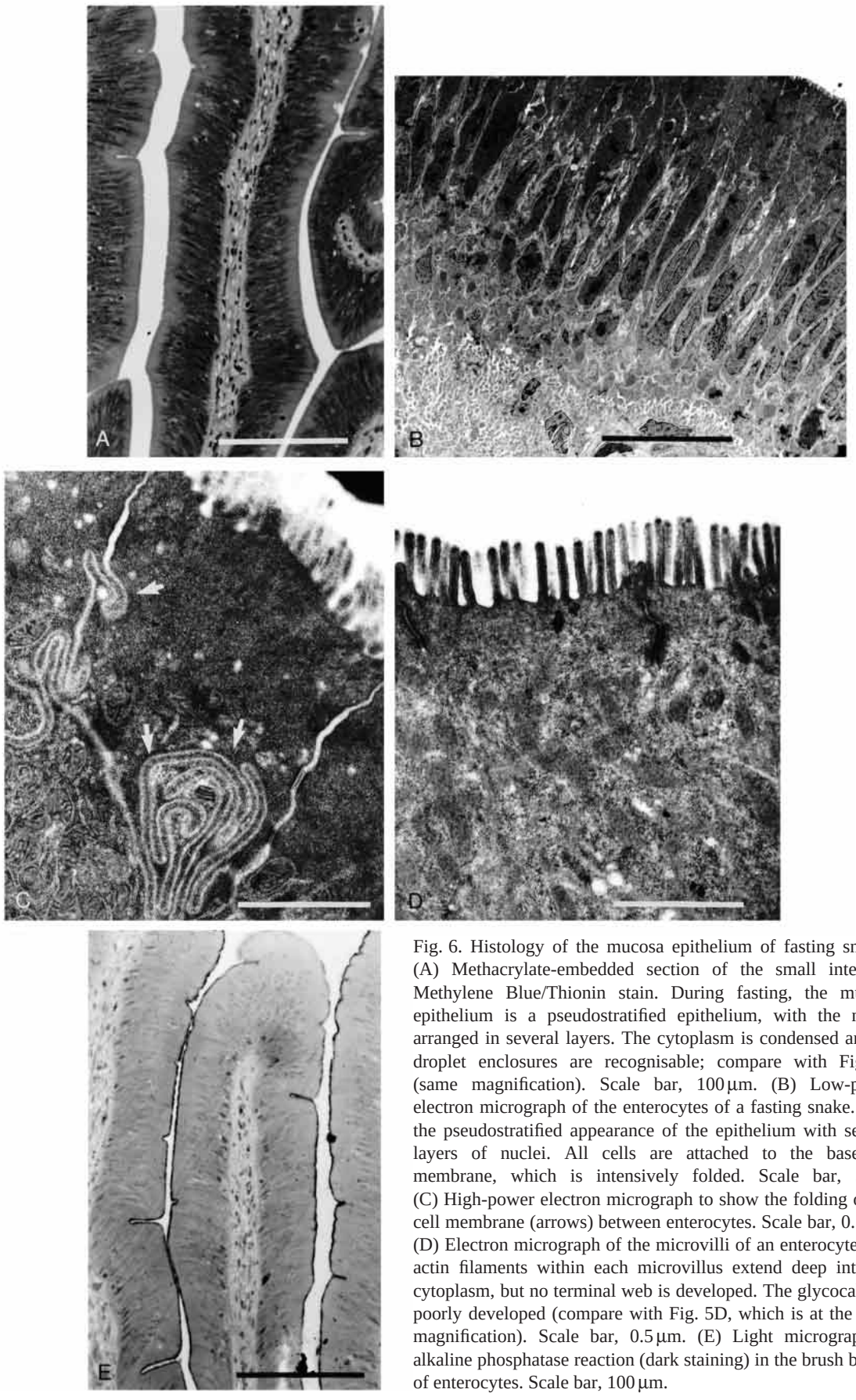

Fig. 6. Histology of the mucosa epithelium of fasting snakes. (A) Methacrylate-embedded section of the small intestine; Methylene Blue/Thionin stain. During fasting, the mucosa epithelium is a pseudostratified epithelium, with the nuclei arranged in several layers. The cytoplasm is condensed and no droplet enclosures are recognisable; compare with Fig. 5A (same magnification). Scale bar, 100 µm. (B) Low-power electron micrograph of the enterocytes of a fasting snake. Note the pseudostratified appearance of the epithelium with several layers of nuclei. All cells are attached to the basement membrane, which is intensively folded. Scale bar, 5 µm. (C) High-power electron micrograph to show the folding of the cell membrane (arrows) between enterocytes. Scale bar, 0.5 µm. (D) Electron micrograph of the microvilli of an enterocyte. The actin filaments within each microvillus extend deep into the cytoplasm, but no terminal web is developed. The glycocalyx is poorly developed (compare with Fig. 5D, which is at the same magnification). Scale bar, 0.5 µm. (E) Light micrograph of alkaline phosphatase reaction (dark staining) in the brush border of enterocytes. Scale bar, 100 µm.

Unlike mammals or birds, pythons have no intestinal crypts. Instead, we found shallow grooves between the villi. Goblet cells were found in small numbers only. The connective tissue core of the villi (lamina propria mucosae) contains smooth muscle cells, large lymphatic spaces (lacteals) and blood vessels. Numerous mast cells loaded with vesicles and lymphocytes are a conspicuous feature of the lamina propria mucosae and were found in all sections of digesting pythons. These migrating cells may also break through the basement membrane of the mucosal epithelium and may occur between the enterocytes.

In fasting pythons, the mucosal epithelium was pseudostratified, with numerous layers of nuclei (Fig. 6A). Transmission electron microscopy revealed that all epithelial cells were in contact with the basement membrane (Fig. 6B), while their nuclei were arranged in several layers (thereby creating the typical appearance of a pseudostratified epithelium). No lipid droplets were found within the body of the cells. The brush border of enterocytes was barely recognizable by light microscopy, and the activity of brush-border alkaline phosphatase was low compared with that of digesting snakes (Fig. 6E). Microvilli were short and bulky, as shown in transmission electron micrographs. The core of actin filaments was present, but did not end in a terminal web as in digesting snakes. Instead, the bundles of actin filaments reached deep into the body of the enterocyte (Fig. 6D). The cytoplasm was dense in the apical part of the enterocytes, and mitochondria had accumulated around the nucleus. The cell membrane of enterocytes was folded, forming spirals of double membranes between neighbouring cells (Fig. 6C). Paracellular channels were absent. The basement membrane of the mucosal epithelium was folded and formed a thick and irregular extracellular lamina. The connective tissue core of the villi was dense, with few small capillaries and no recognizable lacteals as in the digesting snakes.

Cell proliferation

Counts of mitotic structures on histological slides provide a reliable measure of cell proliferation activity. Surprisingly, we were unable to detect any mitosis in the histological sections of the mucosal epithelium of either fasting or digesting snakes (i.e. 2 days after feeding, shortly before maximum the size of the intestine).

Flow cytometry

Two days after feeding, 2.3 % of the cells in the tissue sample were in S-phase. This increased slightly to 3.7 % after 4 days, 3.3 % after 7 days and 3.8 % after 10 days. In fasting snakes, 1.65 % of all cells of the sample were in S-phase (Fig. 7). Analysis of fasting snakes was complicated by the high portion of doublet and quadruplet nuclei, which probably inflated the number of S-phase cells. The data are from six independent flow cytometry runs per day after feeding, but only two individuals per day. Therefore, despite having confidence in the measured values, it would not be reasonable to perform statistical tests on such small sample sizes. However, together with the mitosis counts indicating a complete absence of mitosis in fasting snakes and 2 days after feeding, we believe that cell proliferation rates are low immediately after feeding but increase when organ size has already passed its maximum.

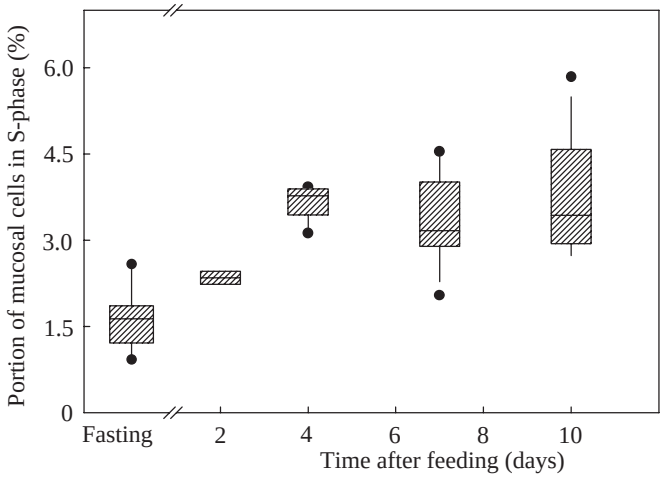

Fig. 7. Results of flow cytometry: relative proportion of S-phase cells in the intestinal wall of fasting snakes (at least 3 months after the last meal) and at successive days after feeding. Values are means of six measurements of two individuals per day. We analyzed S-phase cells instead of G2-phase cells because G2 cell counts might be inflated by nuclei sticking together (see Materials and methods). Box-and-whisker-plot, with horizontal lines showing the 25th, 50th and 75th percentiles as lines on the box, the fifth and the 95th percentiles as error bars (whiskers) and outliers (circles).

Apoptosis

On all slides, apoptotic cells in mouse intestinal tissue provided a positive control and proved that the immunohistochemical test was functional. Also, we were able to detect single apoptotic fibrocytes in the connective tissue (lamina propria mucosae) of the python, indicating that this method was indeed working with python tissue. However, not a single apoptotic enterocyte was found in fasting or digesting snakes using cytoplasmatic markers (transglutaminase) or the nick-end labelling technique. Flow cytometry seemed to be most sensitive to apoptotic cells. In tissue samples from fasting snakes, 5.9 % of the cells were apoptotic. After feeding, the proportion of apoptotic cells increased rapidly to 10.1 % after 2 days, 11.7 % after 5 days, 7.5 % after 7 days and 9.1 % after 10 days. Data are from the same flow cytometry runs as for cells in S-phase (statistical analyses were not performed because of the small sample size). However, these findings provide qualitative evidence that the number of apoptotic cells increases rapidly after feeding, a highly unexpected results given the size increase of the small intestine.

Discussion

Reversability and repeatability

Previous studies (Secor et al., 1994; Secor and Diamond,

1995) showed that the internal organs of Burmese pythons responded to feeding by upregulation of organ size and function followed by downregulation when digestive processes had ended. These findings arose from dissections of young animals. Because an animal cannot be killed twice, the results were derived from different animals and inferences were based on the assumption that all individuals responded in the same manner. Our study is the first to employ noninvasive imaging techniques to investigate the repeatability and reversibility of organ size changes of individual animals under fluctuating conditions. We showed that the size changes of the small intestine mucosa were fully reversible and could be elicited repeatedly in the same individuals. Within 2–3 days of feeding, the thickness of the mucosa peaked at 300 % of fasting size. For small intestine fresh mass, Secor and Diamond reported the same range of change and the same short response time (Secor and Diamond, 1995). Downregulation took longer than upregulation. Ten days after feeding, the mucosa thickness was still 10 % larger than in the fasting condition. On an individual level, the period required to return to fasting size was variable. Size changes occur through elongation of villi and incorporation of lipid droplets into enterocytes. In addition, the microvilli of the brush border elongate and enlarge the absorptive surface area with membrane-bound nutrient transporters.

From a comparative perspective, the rate of size increase of the small intestine is remarkably high. The small intestine of endothermic mammals and birds responds to changes in diet quality and amount of food (for a review, see Starck, 1999). However, size changes do not exceed a factor of 2–2.5, and it takes much longer to upregulate organ size. The flexibility of small intestine size in birds and mammals is based on cellular turnover of the tissue. Turnover rates of between 4 days and 2 weeks have been reported for the small intestine (Starck, 1996a; Starck, 1996b). In addition, a constant high basal metabolic rate and frequent feeding of moderate meal sizes are necessary to sustain such an energetically costly system. How can exothermic pythons increase their small intestine size by a factor of 3 within 2 or 3 days?

A cellular model of flexibility

The peculiar histological features of the python's small intestine provide insights into the mechanism that drives the flexibility of the python gut. First, the mucosal epithelium undergoes considerable changes in cell arrangement and cell size, depending on nutritional state. During fasting, the epithelium is pseudostratified, the enterocytes contain no lipid droplets and the cell membranes of neighbouring cells are folded. When digesting, the mucosal epithelium is single-layered with highly prismatic enterocytes heavily loaded with lipid droplets. The enterocytes are considerably larger than in the fasting condition, the cell membrane is stretched, no spiral foldings of the cell membrane are seen and wide paracellular channels open between the enterocytes. These histological changes are closely associated with a significant increase in villus length. Thus, the mucosal epithelium combines the characteristics of a transitional epithelium with the histological appearance of a pseudostratified epithelium.

Transitional epithelia are usually found in the context of considerable organ size changes. The best known example is in the mammalian urinary system. Filling and emptying of the bladder cause considerable volume changes and, concurrently, distention or relaxation of the bladder epithelium. In the relaxed condition, it consists of several cell layers. In the stretched condition, the positions of the cells change to accommodate the distention of the organ, and the epithelium becomes two-layered (e.g. Bloom and Fawcett, 1986). The mucosal epithelium of the python's small intestine differs from the epithelium of the mammalian urinary tract because it is single-layered. It has no specialized cover cells as in the transitional epithelium in the mammalian bladder. Flexible positions of the cells in an epithelium are a simple solution to accommodate large size changes of an organ without any new tissue production.

Second, during digestion, we found large lymphatic spaces and blood vessels in the connective tissue core of the intestinal villi. Recent duplex-ultrasonography data (J. M. Starck, unpublished data) show that enlarged blood and lymphatic vessels occur in association with increased blood flow to the small intestine after feeding. Therefore, we suggest that a simple fluid pressure pump inflates the intestinal villi to their functional length in response to feeding. Pseudostratified enterocytes would then slide passively into position, forming a single-layered epithelium. In addition, the wide intercellular spaces found between enterocytes in digesting pythons suggest that paracellular nutrient transport contributes to filling the lacteals. Also, the loading of the enterocytes with vesicles suggests that an increase in enterocyte size may contribute to the lengthening of the intestinal villi.

If size changes of the python's small intestine are driven by a fluid pressure pump, we still need to account for the 40 % increase in mass of the small intestine (Secor et al., 1994; Secor and Diamond, 1995). The incorporation of large numbers of lipid droplets into the enterocytes provides a straightforward explanation for the rapid increase in wet and dry mass of the small intestine soon after feeding. So what causes the mass increase is not the production of new tissue but rather the temporary incorporation of lipids into the intestinal tissue.

Third, during the upregulation of organ size, the level of cell proliferation is not increased. In contrast, levels of cell proliferation increase during the subsequent downregulation of organ size: the highest levels of cell proliferation were found when organ size had already passed its maximum size. Thus, organ size changes cannot be driven by hyperplasy (i.e. an increase in cell number). The elevated levels of cell proliferation approximately 1 week after feeding need further explanation. We suggest the following: immediately after feeding, the absorptive surface area of the small intestine is increased by the hypothesised fluid pressure pump system. All enterocytes are active in taking up nutrients from the digesta. At this time, cell proliferation and renewal of the epithelium is neither necessary nor useful, because all cells are functional

and engaged in nutrient uptake. However, nutrient absorption seems to be a process during which cells easily deteriorate. Replacement of cells that deteriorate during nutrient absorption will become necessary when absorption rates decline, i.e. approximately 1 week after feeding. The snake can then await the next meal with a resting, but potentially fully functional, small intestine.

Fourth, at the ultrastructural level, we found considerable changes in the length of the microvilli associated with digestion and fasting. It is difficult to assess what proportion of these changes is based on the production of new cell components. The long extensions of the actin filaments of the microvilli into the cytoplasm during fasting and the weak expression of the terminal web suggest that after feeding the actin filaments extend, thereby stretching and elongating the microvilli before becoming anchored in the terminal web.

Where to pay and when to pump

The pay-before-pumping model (Secor and Diamond, 1995) did not resolve whether SDA immediately after feeding represents the allocation of energy to gastric processes (production of gastric acids and enzymes, activation of nutrient transporters) and/or to the cellular reconstruction of the small intestine. It has been widely perceived from these studies, that 'organ growth and enzyme and transporter synthesis require biosynthetic energy', and that 'high relative costs of digestion are related to biosynthetic start-up costs (...) of synthesizing organs' (Secor and Diamond, 1998, p. 660). With respect to the small intestine, the potential corollaries of the pay-before-pumping model are (i) the high energetic costs of building up a functional organ before a meal can be digested, (ii) that starved animals with depleted energy reserves will not be able to reconstruct their gut, (iii) that the observed rapid size changes of the gut require unphysiologically high proliferation rates and extremely short cell cycle rates and (iv) that, with 25 % of all enterocytes dividing, the absorptive surface of the gut would be greatly reduced.

We have not studied the gastric responses and the energy requirements of postfeeding upregulation of the small intestine. However, the functional histological and morphological results presented here suggest a very fast and immediate response of gut morphology to feeding at no energetic cost for tissue production (because all tissue is present and no biosynthesis is involved). This does not exclude the possibility that energy is required for the upregulation of enzymes and transporters associated with digestive function. Almost all enterocytes are available for absorption instead of a major proportion of the intestinal epithelial cells being allocated to cell division and the production of new tissue. Worn-out cells are replaced when the probability of using them is lower, i.e. when the meal has been absorbed and when the chance of striking another prey is low. This cellular mechanism is fast and energetically cheap. It allows upregulation of the intestine even if the individual is energetically exhausted. It is likely that the mass increase of the small intestine after feeding (Secor and Diamond, 1994) is due to incorporation of lipid droplets into the enterocytes, and is therefore a consequence of, but not the cause of, organ size changes. In an evolutionary although somewhat speculative perspective, the transitional epithelium represents a fast and cheap system that allows upregulation of organ size fairly independently of the energetic condition of the organism. With respect to the size of the small intestine, it seems that the pay-before-pumping model does not apply; instead, the transitional properties of the mucosal epithelium allow for a pump first, pay later mechanism. Such a mechanism may have a considerable selective advantage because it allows for long periods of fasting and depletion of energy reserves, while still enabling the snake to digest prey and absorb nutrients rapidly following a meal. The pay-before-pumping strategy does not allow the snake to make use of all its energy reserves, and the snake could ultimately fall into an energy trap, with its energy stores too exhausted to build up the organ required to gain new energy. In such a case, the snake might starve to death with its stomach full of prey but its energy stores depleted and therefore not enough power available to build up a new intestine to allow digestion of its prey.

The peak metabolic rates recorded 1–2 days after feeding (Secor et al., 1994; Overgaard et al., 1999) require an explanation. Generally, digestion and nutrient transport across the epithelium are metabolically expensive processes that will account for most of the increase in metabolic rates. Also, our study suggests that most of the SDA is probably allocated to upregulation of gastric function, upregulation of transporters and absorptive processes.

Comparative aspects

Plasticity of organ size in response to feeding or changes in food quality has been described in a number of vertebrates (for a review, see Starck, 1999). For birds and mammals, it is well established that small intestine plasticity, in particular size changes of the mucosal epithelium, are based on the permanent production of new enterocytes in the intestinal crypts and on tissue turnover (Sakata and von Engelhardt, 1983; Starck, 1999). Estimates of cell proliferation rates suggest tissue turnover times between 4 days and 2 weeks (Starck, 1996a; Starck, 1996b). We assume that frequent feeding of comparatively small meals requires a permanent rejuvenation of the mucosal epithelium. At the same time, continuous cell proliferation in the intestinal crypts and apoptosis at the tip of the villi provide a mechanism for fast responses to changes in diet. However, details of the cellular mechanism that regulates up- and downregulation of mucosal epithelium, i.e. the balance between cell proliferation and apoptosis, are more-or-less unknown (Sakata and von Engelhardt, 1981; Sakata and von Engelhardt, 1983; Lupton et al., 1988; von Engelhardt et al., 1989; Wang et al., 1991; Enns et al., 1994; Enns et al., 1996; Hammond et al., 1996). The peculiar cellular mechanism that drives the plasticity of the small intestine of pythons as described here is unique and unknown in other vertebrates. Therefore, generalizations based on the python's gut as a vertebrate model of extreme physiological regulation (Secor and Diamond, 1998) may require down-tuning because the

python gut actually represents a rather specialized 'bladder-like' mechanism.

Thomas Hildebrandt and Frank Göritz, Institute of Zoo- and Wildlife Biology, Berlin, took the microbiopsy samples. We gratefully acknowledge their exceptional veterinarian skills and sophisticated knowledge of exotic animal diagnostics and treatments. We would like to thank Anja Burann and Sybille Koch for technical help in the laboratory and dedicated management of the snakes. We thank Andrea Klein, Giessen, for preparing transmission electron microscopy samples, Andreas Aschoff, Jena, for apoptosis immunohistochemistry and Ruedi Braun, Jena, for providing access to the flow cytometry laboratory. We are grateful to Barbara Helm, MPI Andechs, Theunis Piersma, NIOZ Texel, and Stephen Secor, University of Mississippi, for comments and suggestions on an earlier version of the manuscript. The study was supported by the German Research Council (DFG) grants STA 345/2-2, 345/4-1 and 345/5-1 and a grant of the German Ornithological Society.

References

Aschoff, A., Jantz, M. and Jirikowski, G. F. (1996). In-situ end labeling with bromodeoxyuridine – an advanced technique for the visualization of apoptotic cells in histological specimens. *Horm. Metab. Res.* **28**, 311–314.

Aschoff, A. and Jirikowski, G. F. (1997). Apoptosis: Correlation of cytological changes with biomedical markers in hormone-dependent tissues. *Horm. Metab. Res.* **29**, 535–543.

Bancroft, J. D. and Stevens, A. (1996). *Theory and Practice of Histological Techniques*. Fourth edition. New York: Churchill Livingstone.

Bloom, D. W. and Fawcett, M. D. (1986). *A Textbook of Histology*. Eleventh edition. Philadelphia: Saunders Company.

Cossins, A. R. and Roberts, N. (1996). The gut in feast and famine. *Nature* **376**, 23.

Dietz, M., Dekinga, W., Piersma, T. and Verhulst, S. (1999). Estimating organ size in small migrating shorebirds with ultrasonography: an intercalibration exercise. *Physiol. Biochem. Zool*. **72**, 551–557.

Enns, M. L., Schmidt-Wittig, U., Müller, H., Mai, U. E. H. Coenen, M., Gärtner, K. and Hedrich, H. J. (1994). Orally applied endotoxin stimulates colonic mucin releasing cells in germfree rats. *J. Exp. Anim. Sci.* **37**, 138–148.

Enns, M. L., Schmidt-Wittig, U., Müller, H., Mai, U. E. H., Coenen, M. and Hedrich, H.J. (1996). Response of germfree rat colonic mucous cells to peroral endotoxin application. *Eur. J. Cell Biol*. **71**, 99–104.

Hammond, K. A., Lam, M., Lloyd, K. C. and Diamond, J. M. (1996). Simultaneous manipulation of intestinal capacities and nutrient loads in mice. *Am. J. Physiol*. **271**, G969–G979.

Hildebrandt, T. B., Göritz, F., Stetter, M. D., Hermes, R. and Hofmann, R. R. (1998). Applications of sonography in vertebrates. *Zoology* **101**, 200–209.

Lupton, J. R., Coder, D. M. and Jacobs, L. R. (1988). Long-term effects of fermentable fibers on rat colonic pH and epithelial cell cycle. *J. Nutrit.* **1**, 840–845.

Overgaard, J., Busk, M., Hicks, J. W., Jensen, F. B. and Wang, T. (1999). Respiratory consequences of feeding in the snake *Python molurus*. *Comp. Biochem. Physiol*. **124**A, 359–365.

Piersma, T. and Lindström, A. (1997). Rapid reversible changes in organ size as a component of adaptive behavior. *Trends Ecol. Evol.* **12**, 134–138.

Sakata, T. and von Engelhardt, W. (1981). The influence of short-chain fatty acids and osmolality on mucin release in the rat colon. *Cell Tissue Res.* **219**, 371–377.

Sakata, T. and von Engelhardt, W. (1983). Stimulatory effect of short chain fatty acids on the epithelial cell proliferation in rat large intestine. *Comp. Biochem. Physiol.* **74**A, 459–462.

Secor, S. M. (1995). Digestive response to the first meal in hatchling Burmese pythons (*Python molurus*). *Copeia* **1995**, 947–954.

Secor, S. M. and Diamond, J. (1995). Adaptive responses to feeding in Burmese pythons: pay-before-pumping. *J. Exp. Biol.* **198**, 1313–1325.

Secor, S. M. and Diamond, J. (1997). Determinants of the postfeeding metabolic reponse of Burmese pythons, *Python molurus*. *Physiol. Zool*. **70**, 202–212.

Secor, S. M. and Diamond, J. (1998). A vertebrate model of extreme physiological regulation. *Nature* **395**, 659–662.

Secor, S. M., Stein, E. D. and Diamond, J. (1994). Rapid upregulation of snake intestine in response to feeding: a new model of intestinal adaptation. *Am. J. Physiol.* **266**, G695–G705.

Starck, J. M. (1996a). Phenotypic plasticity, cellular dynamics and epithelial turnover of the intestine of Japanese quail (*Coturnix coturnix japonica*). *J. Zool., Lond.* **238**, 53–79.

Starck, J. M. (1996b). Intestinal growth in altricial European starling (*Sturnus vulgaris*) and precocial Japanese quail (*Coturnix coturnix japonica*). A morphometric and cytokinetic study. *Acta Anat.* **156**, 289–306.

Starck, J. M. (1999). Structural flexibility of the gastro-intestinal tract of vertebrates. Implications for evolutionary morphology. *Zool. Anz.* **238**, 87–101.

Starck, J. M. and Burann, A. K. (1998). Noninvasive imaging of the gastrointestinal tract of snakes: A comparison of normal anatomy, radiology and ultrasonography. *Zoology* **101**, 210–223.

Starck, J. M., Dietz, M., and Piersma, T. (2001). Ultrasound scanning. In *Body Composition Analysis: A Handbook of Non-Destructive Methods* (ed. J. R. Speakman). Cambridge: Cambridge University Press (in press).

von Engelhardt, W., Rönnaui, K., Rechkemmer, G. and Sakata T. (1989). Absorption of short-chain fatty acids and their role in the hindgut of monogastric animals. *Anim. Feed Sci. Technol.* **23**, 43–53.

Wang, J. Y., McCormack, S. A., Viar, M. J. and Johnson, L. R. (1991). Stimulation of proximal small intestinal mucosal growth by luminal polyamines. *Am. J. Physiol*. **261**, G504–G511.

Weibel, E. R., Taylor, C. R. and Bolis, L. (1998). *Principles of Animal Design. The Optimization and Symmorphosis Debate.* Cambridge: Cambridge University Press.